Title
THE CHARACTERIZATION OF THE DAMAGE INTRODUCED DURING MICRO-EROSION OF MgO SINGLE CRYSTALS

Author
Narayan, J.

Publication Date
1973

Submitted to Wear

LBL-887
Preprint

THE CHARACTERIZATION OF THE DAMAGE INTRODUCED DURING MICRO-EROSION OF MgO SINGLE CRYSTALS

J. Narayan

January 1973

Prepared for the U. S. Atomic Energy Commission
under Contract W-7405-ENG-48

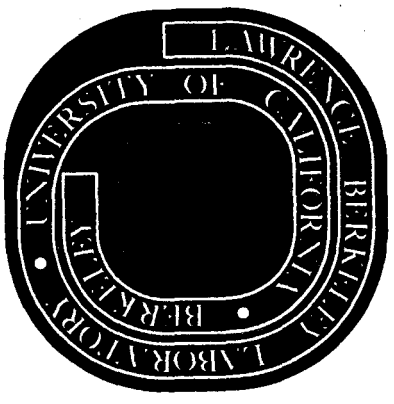

DISCLAIMER

LBL-887

THE CHARACTERIZATION OF THE DAMAGE INTRODUCED DURING MICRO-EROSION OF MgO SINGLE CRYSTALS

J. Narayan*

Inorganic Materials Research Division, Lawrence Berkeley Laboratory and Department of Materials Science and Engineering, College of Engineering; University of California, Berkeley, California

ABSTRACT

The plastic damage introduced in MgO single crystals by bombardment with Al_2O_3 microspheres (0.3, 20 and 27 μ dia) has been studied using optical, transmission and scanning electron microscopy. Most of the damage is in the form of dislocation dipoles (two closely spaced dislocations of opposite sign) which lie on {110} slip planes. The dislocation density increases with the increase in the energy of the impinging particles. Using stereo-microscopy the damage has been shown to be uniformly distributed in thin foils. Studies done on indentations produced by a sharp pin show a very high density of single dislocations.

---

*Present address: Solid State Division, Oak Ridge National Laboratory Oak Ridge, Tennessee 37830.

I. INTRODUCTION

Erosion refers to the disintegration of materials due to impinging particulate matter in the form of dusts or other small particles. Erosion is often detrimental, as is evident from recent experiences with turbine engines in helicopters. The cost of maintaining such engines in dusty environments is appreciable. Air filtration has alleviated the problem somewhat, but filtration reduces both payload and engine performance. Erosive action of particles are also used for beneficial purposes. For example, sand blasting techniques are often employed to clean stone or masonry structures and rock cutting.

The basic problem of the designer is to optimise the effects of erosion and to have a fairly good knowledge of erosion rate under a given set of conditions. This requires an understanding of the mechanism of the erosion process; in other words, the nature of the plastic damage introduced during erosion. The theories[1-3] based on macro-experimental facts to predict the erosion rates lack the firm support for the assumptions made.

The purpose of this paper is to present a detailed study on the nature of the plastic damage produced during erosion. The preliminary results have already been reported.[4]

II. EXPERIMENTAL

Magnesium oxide in form of large grains had the following impurities in PPM: Al-200; Si-200; F-30. Thin {100} slices were obtained by cleaving large grains along {100} faces. The surface damage was removed by chemical polishing in hot (150-160°C) phosphoric acid. Thinning was continued from both sides to a thickness of about 0.05 cm. These thin crystals were then etched in the solution, 5 parts of saturated ammonium chloride, 1 part of sulfuric acid and 1 part distilled water, at room temperature for about 15 min. Conical pits develop where dislocations emerge through surfaces. Dislocation free areas were bombarded from one side by Al_2O_3 particles of 0.3, 20 and 27 μ in diameter, at about 80° from the (001) surface of the crystal using a pressurized gun at 65 lbs. The crystals were cleaned by air, distilled water and methyl alcohol and then re-etched. The plastic damage was examined by optical microscopy, scanning electron microscopy and transmission electron microscopy in accordance with the following techniques:

(i) Optical microscopy: A Zeiss optical microscope was used. After etching, the plastic damage in the regions hit by particles is revealed in the microscope.

(ii) Scanning electron microscopy: since MgO is non-conducting, a thin conducting layer was needed to examine the samples in the scanning electron microscope. A thin layer of aluminum (∿ 80 Å) was deposited on samples which were already etched. A JSM-U3 scanning electron microscope was used to make observations.

(iii) Transmission electron microscopy: bombarded samples were cleaned by the method described above and then chemically polished from the unbombarded side using a jet polishing technique.[5] A thin region for transmission electron microscopy was cut along ⟨100⟩ by a blade. A 100 keV Siemens and the Berkeley 650 keV Hitachi microscope were used. The high voltage microscopy is superior in resolution, penetration thickness and lens aberrations to the low voltage microscope.

In another set of experiments, a given area of a thin foil was first photographed using transmission electron microscopy and then the same area was bombarded and rephotographed. This way one can be sure of initial dislocation density. Stereo microscopy was done to find the depth distribution of the plastic damage. The annealing of the damage either by heating the samples outside or by removing the condenser aperture was also studied.

The plastic damage was also introduced in thin crystals (1×1×.05 cm) by indenting with a sharp pin. These crystals were polished from the other side and examined in the microscope.

III. RESULTS

MgO has six $\{110\}\langle 1\bar{1}0\rangle$ slip systems, four $((101)[\bar{1}01]$, $(\bar{1}01)[101]$ and $(011)[0\bar{1}1]$, $(0\bar{1}1)[011])$ at 45 degrees to the (001) surface (henceforward to be referred as $(101)_{45°}$ and $(011)_{45°}$) and two $((110)[\bar{1}10]$, $(\bar{1}10)[110]$ at 90 degrees to the (001) surface (henceforward to be referred as $(110)_{90°}$ planes).

Figure 1a is an optical micrograph of (001) surface which has been bombarded by 0.3 μ particles at about 85 degree from the surface and subsequently etched. Near the points A, B, C and D there is a "rosette" shaped structure, showing the slip on {110} planes. Dark contrast in the

center is due to some erosion of the surface. Since the particles were bombarded at ~85° from the (001) surface, the resolved stresses on $(110)_{90°}$ planes are very small. That is why "rosettes" are more elongated along [100] and [010] directions than along [110], [$\bar{1}$10] directions. When the deformed crystal is viewed along [001] direction, the plastic damage on (011)[0$\bar{1}$1] and (0$\bar{1}$1)[011] slip systems is projected along [100] direction, and the damage on (101)[$\bar{1}$01] and ($\bar{1}$01)[101] slip systems along [010] direction. However, the damage on (110)[$\bar{1}$10] and ($\bar{1}$10)[110] slip systems is projected along [$\bar{1}$10] and [110] directions respectively. Figure 1b shows the optical micrograph of the (001) surface bombarded by 27 μ particles at about 75 degrees from the surface and then etched. In this case "rosettes" are revealed clearly because slip is occurring in all six {110}⟨$\bar{1}$10⟩ slip systems. These optical observations are similar to those of Stokes, Johnston and Li in MgO.[5]

Figure 2a is the scanning electron micrograph of the surface shown in Fig. 1a. At points A, B and C micro-erosion and associated slip is revealed. Figure 2b shows the surface after being bombarded by 27 μ particles. At A, B and D (Fig. 2b) there is both slip and erosion but at point C there is only slip and no erosion. Notice the crack at the point A.

The plastic damage increases as the size of the particles increases. Figure 3a is an electron micrograph (100 kV) for 0.3 μ particles using the diffraction vector g = [200], the damage on $(110)_{90°}$ and $(101)_{45°}$ planes is in contrast. Figure 3b shows the same area for g = [020], revealing the damage on $(110)_{90°}$ and $(011)_{45°}$ planes. Notice the disappearance of the camage in $(101)_{45°}$ planes in Fig. 3b. Figure 4a is a 100 kV electron micrograph for 27 μ particles for g = 200. Figure 4b is the same area for

g = [020]. Notice the disappearance of the damage on $(101)_{45°}$ plane in Fig. 4b. The damage on $(110)_{90°}$ planes is less because the direction of bombardment is very close to [001] direction. Notice the higher dislocation density in Fig. 4 than that in Fig. 3.

Figures 5 through 7 are 65° kV high voltage micrographs. Figure 5a is for the diffraction vector g = [200], revealing the damage on $(110)_{90°}$ planes and $(101)_{45°}$ planes for 10 μ particles. The damage along [110] and $[\bar{1}10]$ is on $(110)_{90°}$ planes and that along $[0\bar{1}0]$ is on $(101)_{45°}$ planes. The smaller dislocation density on $(110)_{90°}$ planes is due to less resolved shear stress along [110] and $[\bar{1}10]$ directions, the direction of bombardment being close to [001]. Figure 5b shows another area for g = [200], revealing the damage on $(110)_{90°}$ and $(101)_{45°}$ planes. At point A in Fig. 5b, the particle (20 μ) hit, but the nearby area was dislocation free because the damage popped out of the surface from the other side during polishing. Figure 6a for g = [020] shows how the damage (20 μ) from two sources meets along A-A. In Fig. 6b, particles probably hit at C and D where very dense slip on $(011)_{45°}$ started. Notice the relatively small damage on $(110)_{90°}$ planes. Figure 7a (27 μ particles) is for the diffraction vector g = [020], therefore the damage on $(110)_{90°}$ and $(011)_{45°}$ planes is in contrast. Probably the particle hit at A where dense slip started. Again notice the relative small damage on $(110)_{90°}$ planes. Figure 7b (27 μ particles) is for the diffraction vector [220], revealing the damage only on $(110)[\bar{1}10]$ slip system; and $(101)_{45°}$ and $(011)_{45°}$ slip planes. Particles probably hit at D, E and F, where there is severe damage.

During polishing the dislocations sometimes are introduced and/or there is rearrangement of the dislocations already present. To test the possibility of such effects, a thin electron microscope foil was first

photographed and then dislocation free areas were bombarded. Figure 8 shows the damage after bombarding with 27 μ particles. The diffraction vector is [220], revealing the damage on the $(\bar{1}10)[110]$ slip system and $(101)_{45°}$ and $(011)_{45°}$ planes. The nature of the plastic damage is similar to that observed in bulk crystals. However due to smaller foil thickness, the observed damage is less.

The plastic damage is uniformly distributed only in the vicinity of the point of impact. It gets shallower with distance from the point of impact. Figure 9 shows the stereo pair at 15° of the damage introduced by bombardment of 27 μ particles. This pair when viewed along maximum parallax direction, i.e., perpendicular to diffraction vector gives three-dimensional distribution. This showed that the damage is uniformly distributed throughout the foil. This was in a thin sample which was prepared from a thick bombarded crystal. Figures 10 and 11 are micrographs from samples which were bombarded with 27 μ particles when they were thin enough for the microscopy. When this foil is annealed at 1100°C for 1 hr outside the electron microscope and rephotographed, most of the damage is annealed out. Some prismatic dislocation loops (A, B, C and D in Fig. 10b) appear, showing that during bombardment point defects are also being produced. Figure 11 shows a series of pictures (a, b and c) where condenser operature was removed. Since MgO is fairly non-conducting, localized temperature might go as high as 900°C and dislocations are lost to the surface. A definite loss of dislocations from Fig. 11a to 11c is apparent. From Figs. 10 and 11, it can be inferred that most of the damage is concentrated at one surface of the foil. The plastic damage observed in Figs. 10 and 11 was from the areas away from point of impact. Therefore the damage is concentrated at the surface of the foil.

Figure 12 shows the damage introduced due to indentations by a sharp pin. Actual indentations are shown at A and B. Most of the damage is in the form of pileups of single dislocations which run from top to bottom of the foil. Also notice the micro-cracks associated with the indentations. When many indentations are made close to each other, pile ups from different sources result. Figure 12c shows the latter where different sources of pileups can be traced.

IV. DISCUSSION

When a ball strikes the surface, the maximum pressure p_o under the area of contact under statical conditions is given by the Hertz theory[7] as:

$$p_o = \frac{3p}{2\pi a^2} \quad , \tag{1}$$

where p is the total compressive force and a is the radius of the area of contact.

a can be expressed as:

$$a = \left[\frac{3}{4} PR \left(\frac{1-\nu_1^2}{E_1} + \frac{1-\nu_2^2}{E_2}\right)\right]^{1/3} \tag{2}$$

or

$$a = \frac{\pi p_o R}{2} \left[\frac{1-\nu_1^2}{E_1} + \frac{1-\nu_2^2}{E_2}\right] \quad , \tag{3}$$

where R is the radius of the ball; ν_1, E_1 and ν_2, E_2 are Poisson's ratios and elastic moduli of the surface and the ball respectively. The duration of impact t has been derived to be

$$t = 2.94 \left[\frac{15}{16} \frac{m_2}{\sqrt{R}} \left(\frac{1-\nu_1^2}{E_1} + \frac{1-\nu_2^2}{E_2}\right)\right]^{2/5} \frac{1}{(u_2)^{1/5}} \tag{4}$$

or

$$t = 2.94 \left[\frac{5\pi\rho}{4} \left(\frac{1-\nu_1^2}{E_1} + \frac{1-\nu_2^2}{E_2}\right)\right]^{2/5} \frac{R}{(u_2)^{1/5}} , \tag{5}$$

where m_2, ρ and u_2 are the mass, density and velocity of the impinging ball respectively.

The total force p can be expressed (using Eqs. 1 through 5) as:

$$p = \left(\frac{5}{4} m_2 u_2^2\right)^{3/5} \left[\frac{4\sqrt{R}}{3\left(\frac{1-\nu_1^2}{E_1} + \frac{1-\nu_2^2}{E_2}\right)}\right]^{2/5} , \tag{6}$$

Therefore the maximum pressure p_o is equal to

$$p_o = \frac{3}{2} \frac{\left(\frac{5}{4} m_2 u_2^2\right)^{1/5}}{R^{3/5}} \left[\frac{4}{3} \left(\frac{1-\nu_1^2}{E_1} + \frac{1-\nu_2^2}{E_2}\right)\right]^{-4/5} \tag{7}$$

or

$$p_o = \frac{3}{2}\left(\frac{5\pi}{3} \rho u_2^2\right)^{1/5} \left[\frac{4}{3} \frac{1-\nu_1^2}{E_1} + \frac{1-\nu_2^2}{E_2}\right]^{-4/5} . \tag{8}$$

The maximum shear stress on which the yielding of a plastic solid depends, is $\left(\frac{1+2\nu_1}{2}\right)p_o$. This occurs at about a/2 along the center line of the ball.

The failure of a perfectly brittle material is determined by the maximum tensile stress. This occurs at the circular boundary of the surface of contact. It acts in the radial direction and has the magnitude $\left(\frac{1-2\nu_1}{3}\right)p_o$. The other principal stress, acting in the circumferential direction, is numerically equal to the above radial stress but of opposite sign.

A complication arises if the impinging ball is not spherical and/or if the flat surface contains dirt particles which can act as stress concentrates.

The estimated particle velocity was in the range of 500 ft/sec. Using $\rho_{MgO} = 3.58$ gm/cm^3, $\nu_{MgO} = 0.3$, $E_{MgO} = 1.3 \times 10^{12}$ dynes/cm^2 and $\rho_{Al_2O_3} = 3.97$ gm/cm^3, $\nu_{Al_2O_3} = 0.254$, $E_{Al_2O_3} = 3.8 \times 10^{12}$ dynes/cm^2, the maximum pressure p_o from Eq. (8) is $\sim 2.0 \times 10^{10}$ dynes/cm^2. The maximum shear and tensile stresses are 1.6×10^{10} dynes/cm^2 and 3.0×10^9 dynes/cm^2. These can be compared with the yield stress along <100> in MgO at room temperature[9] of about 3.0×10^9 cynes/cm^2. In this situation if there are no flaws or sources of stress concentration, the fracture probably cannot occur because the tensile stress is not sufficient to initiate the crack. However, the shear stress is enough to cause the plastic damage in the material and so most of the erosion is occurring by shear cutting typical of a plastic solid.

The total plastic damage estimated from the micrographs after taking into account the foil thickness decreases as the particle size decreases. This is reasonable as the total force p varies as R^2. Therefore, energy transmitted by the impinging particles decreases as the size of the particle decreases. The amount of energy stored in the form of plastic damage is simply dislocation density times energy of the dislocation per unit length plus the interaction energy of dislocations. The nature of the dislocation should

also be taken into account; for example, the dislocations introduced during pin indentation are mostly of screw character. The line energy of an edge dislocation is $1/(1-\nu_1)$ times larger than that of a screw dislocation. The importance of the knowledge of the transmitted energy in developing the theories of erosion has been emphasized by Head and Harr.[6] They showed that steady-state erosion is directly proportional to the energy transmitted from impinging particles to the target. It should be further emphasized that though MgO is a typical brittle solid, when bombarded by small particles (< 27 μ) it is eroded like a plastic solid. This gives a firm support to the probabilistic theory based on flaws, according to which, as the particle size gets smaller, the probability of its encountering a flaw gets lower. Therefore fracture, the mode of failure of a brittle solid, cannot be initiated and the material behaves like a plastic solid. The damage introduced by a sharp pin causes plastic damage and fracture because the end of a sharp pin acts as a stress concentrater. It is interesting to note that most of the plastic damage is stored in the form of dislocation dipoles. This is probably because cross slip is favored at higher strain rates.[10] The duration of impact from Eq. (5) is 2.2×10^{-8} sec. The strain rate produced is of the order of 10^5/sec.

V. CONCLUSION

Magnesium oxide behaves as a plastic solid when bombarded by Al_2O_3 particles < 27 μ. The plastic damage is stored in the form of dislocation dipoles on all $\{110\}\langle\bar{1}10\rangle$ slip systems. The damage has been shown

to be uniformly distributed in thin foils and it increases with the energy of impinging particles. The plastic damage introduced by indentations of sharp pins is mostly in the form of single dislocations or point defects.

ACKNOWLEDGEMENT

This work was done under the auspices of the United States Atomic Energy Commission through the Inorganic Materials Research Division of Lawrence Berkeley Laboratory.

The author is grateful to Prof. J. Washburn for helpful discussions.

REFERENCES

1. G. L. Sheldon, Erosion of Brittle Materials, (D. Eng. Thesis) University of California, Berkeley, California.
2. G. L. Sheldon and I. Finnie, On the Ductile Behavior of Nominally Brittle Materials During Erosive Cutting, paper presented to Winter Meeting of ASME, November, 1965.
3. G. L. Sheldon and I. Finnie, The Mechanism of Material Removal in the Erosive Cutting of Brittle Materials, paper presented to Winter Meeting of ASME, 1965.
4. J. Narayan and J. Washburn, Wear, in press.
5. R. J. Stokes, T. L. Johnston and C. H. Li, Trans. AIME 215, (1959) 437.
6. W. J. Head and M. E. Harr, Wear 15 (1970) 1-46.
7. S. Timoshenko and J. N. Goodier, Theory of Elasticity, 2nd Edition, McGraw-Hill Book Co. Inc., 1951.
8. Lord Rayleigh, Phil. Mag., Series 6, 11 (1906) 283.
9. T. G. Langdon and J. A. Pask, High Temp. Oxides 53, (1970) 3.
10. J. J. Gilman, Micromechanics of Flow in Solids, McGraw-Hill Book Co. Inc., 1969.

FIGURE CAPTIONS

Fig. 1 Optical micrographs: a) surface bombarded by 0.3 μ Al_2O_3 particles at ~ 85° from [001] and subsequently etched; b) surface bombarded by 27 μ Al_2O_3 particles at ~ 75° from [001] and subsequently etched.

Fig. 2 Scanning electron micrographs: a) corresponding to Fig. 1a; b) coresponding to Fig. 1b.

Fig. 3 100 kV transmission electron micrographs for 0.3 μ particles bombarded at 85° from [001]: a) for diffraction vector g = [200]; b) the same area as 'a' for diffraction vector g = [020]. Point A is the same in both pictures.

Fig. 4 100 kV transmission electron micrographs for 27 μ particles bombarded at 85° from [001] direction: a) g = [200]; b) g = [020]. Notice the disappearance of one set of dislocations with $b = \frac{1}{2}[101]$ or $\frac{1}{2}[\bar{1}01]$. Point A is the same in both pictures.

Fig. 5 650 kV transmission electron micrographs a) and b) for 10 and 27 μ particles respectively bombarded at ~ 85° from [001] direction: a) g = [200] shows the damage on $(101)_{45°}$ plane and $(110)_{90°}$ planes; b) g = [200]. Notice the dislocation-free area around A, where a particle hit.

Fig. 6 650 kV transmission electron micrographs for 20 μ particles bombarded in the same way as for Fig. 5. a) g = [020] shows the damage from two sources meeting along A-A; b) g = [020] revealing the damage on $(011)_{45°}$ and $(110)_{90°}$ planes. Particles probably hit at C and D where very dense slip started.

Notice that the majority of the damage is in form of dislocation dipoles.

Fig. 7 650 kV transmission electron micrographs: a) g = [020] reveals the damage due to 27 μ particles on $(110)_{90°}$ and $(011)_{45°}$ planes; b) g = $[\bar{2}20]$ shows the damage due to 27 μ particles on $(110)[\bar{1}10]$ slip system and $(101)_{45°}$ and $(011)_{45°}$ planes. Particles probably hit at A, D and E.

Fig. 8 100 kV transmission electron micrographs of a thin foil after bombardment by 27 μ particles; a and b show the damage on $(\bar{1}10)[110]$ slip system and on $(101)_{45°}$, $(011)_{45°}$ planes.

Fig. 9 Stereo pair at 15° of the damage by 27 μ particles.

Fig. 10 a) The damage in a thin foil after bombardment by 27 μ particles for diffraction vector g = [200]; b) the same foil after annealing at 1100°C for one hour outside the electron microscope. Notice the prismatic dislocation loops A, B, C and D.

Fig. 11 Annealing due to condenser operture removal of the damage introduced by bombardment of 27 μ particles.

Fig. 12 a) Pin indentation at A. Notice the damage around A in the form of dislocations running from top to bottom of the foil. b) Pin indentation at B. Notice the damage in the form single dislocations and associate crack. c) Pile up on dislocations from many sources (pin indentations).

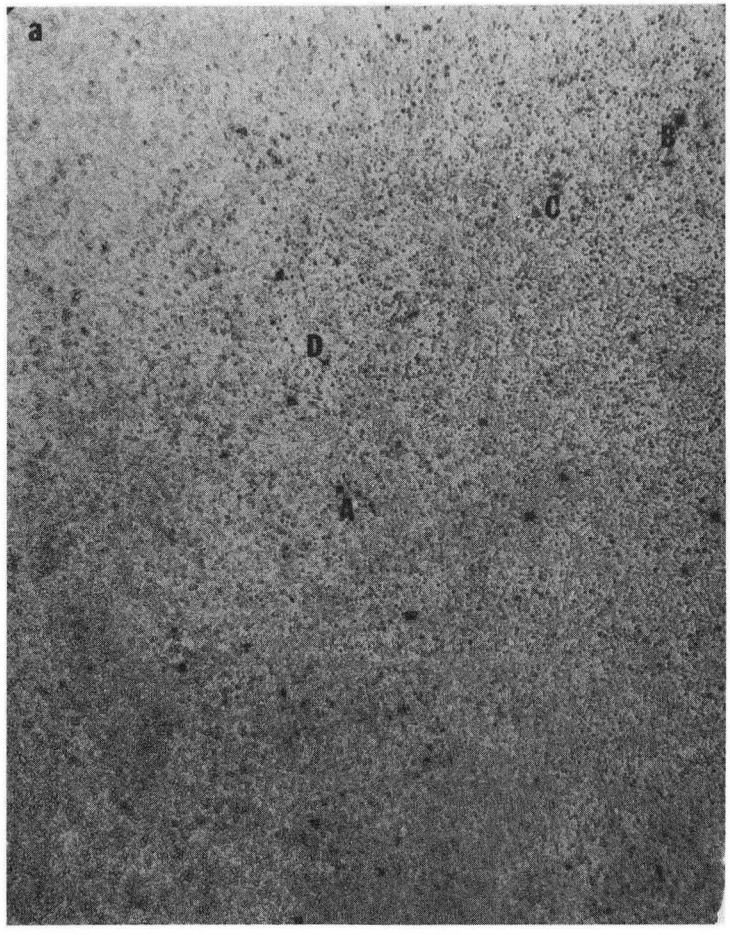

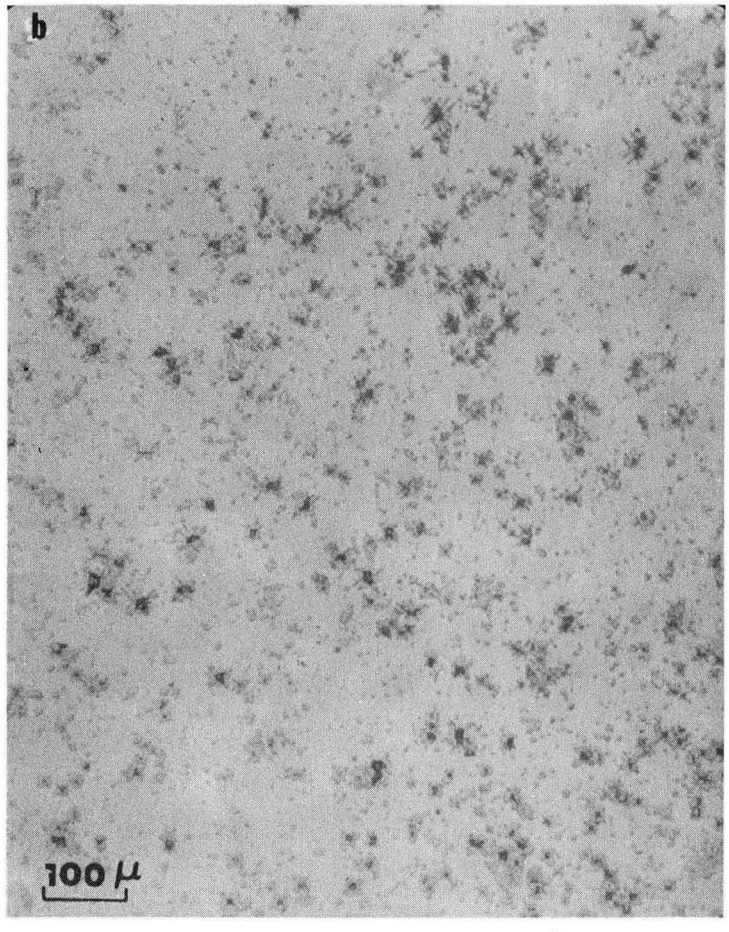

XBB 727-3640

Fig. 1.

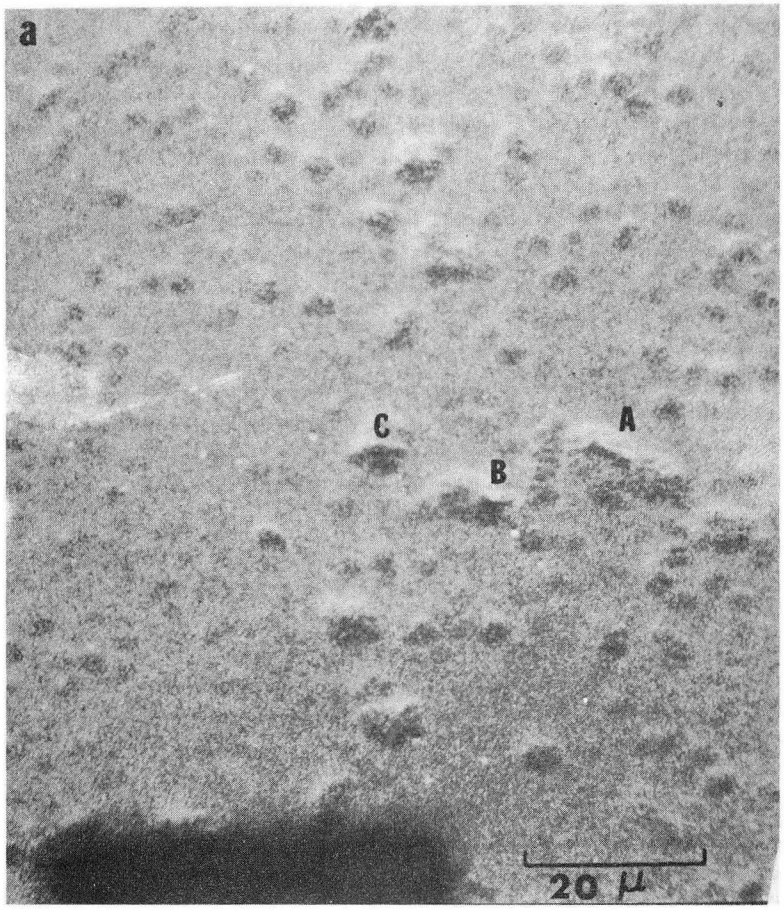

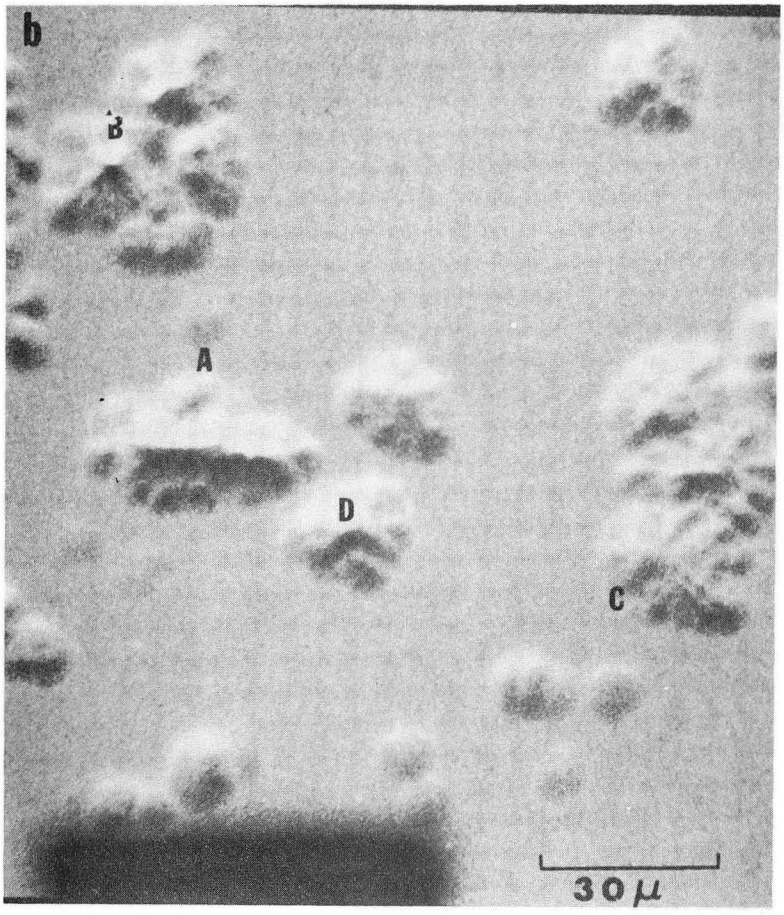

XBB 727-3641

Fig. 2.

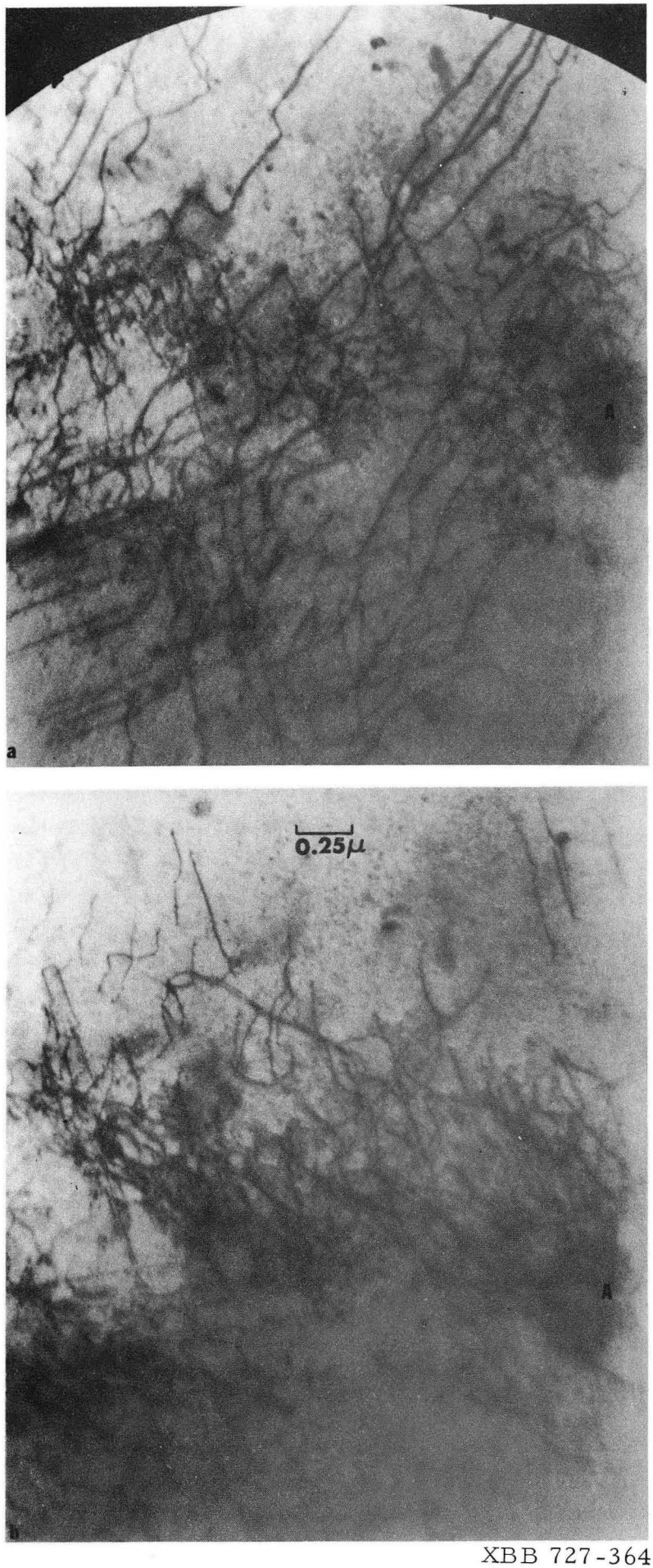

XBB 727-3646

Fig. 3.

XBB 727-3644

Fig. 4.

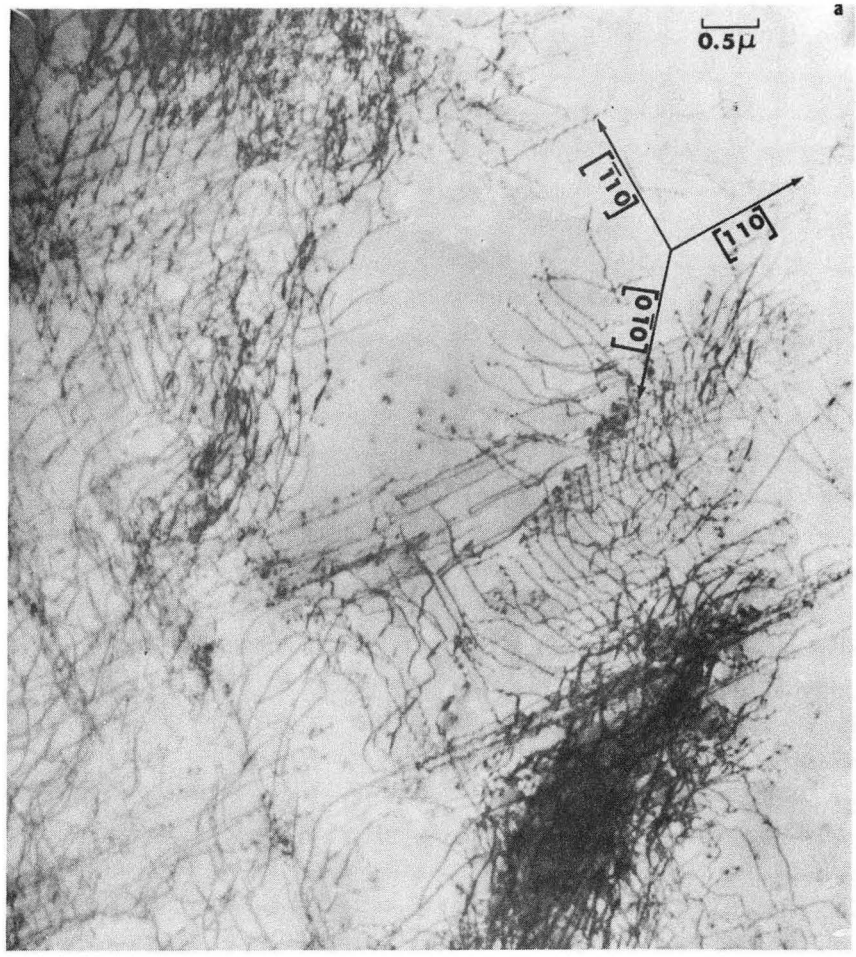

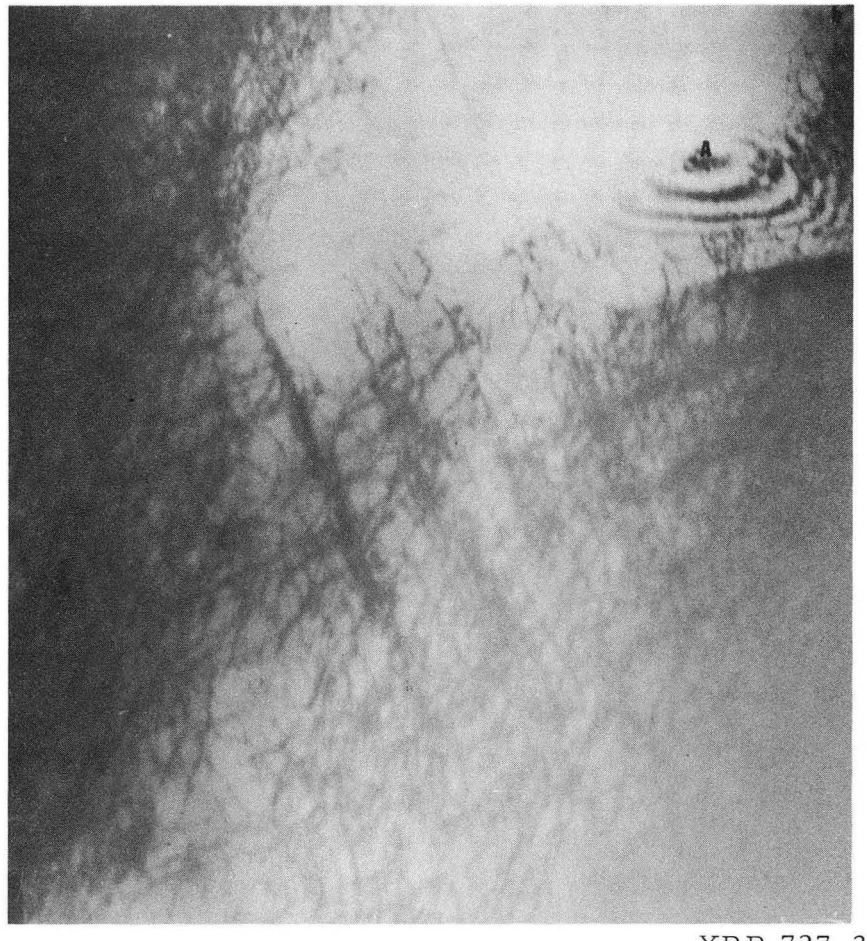

XBB 727-3645

Fig. 5.

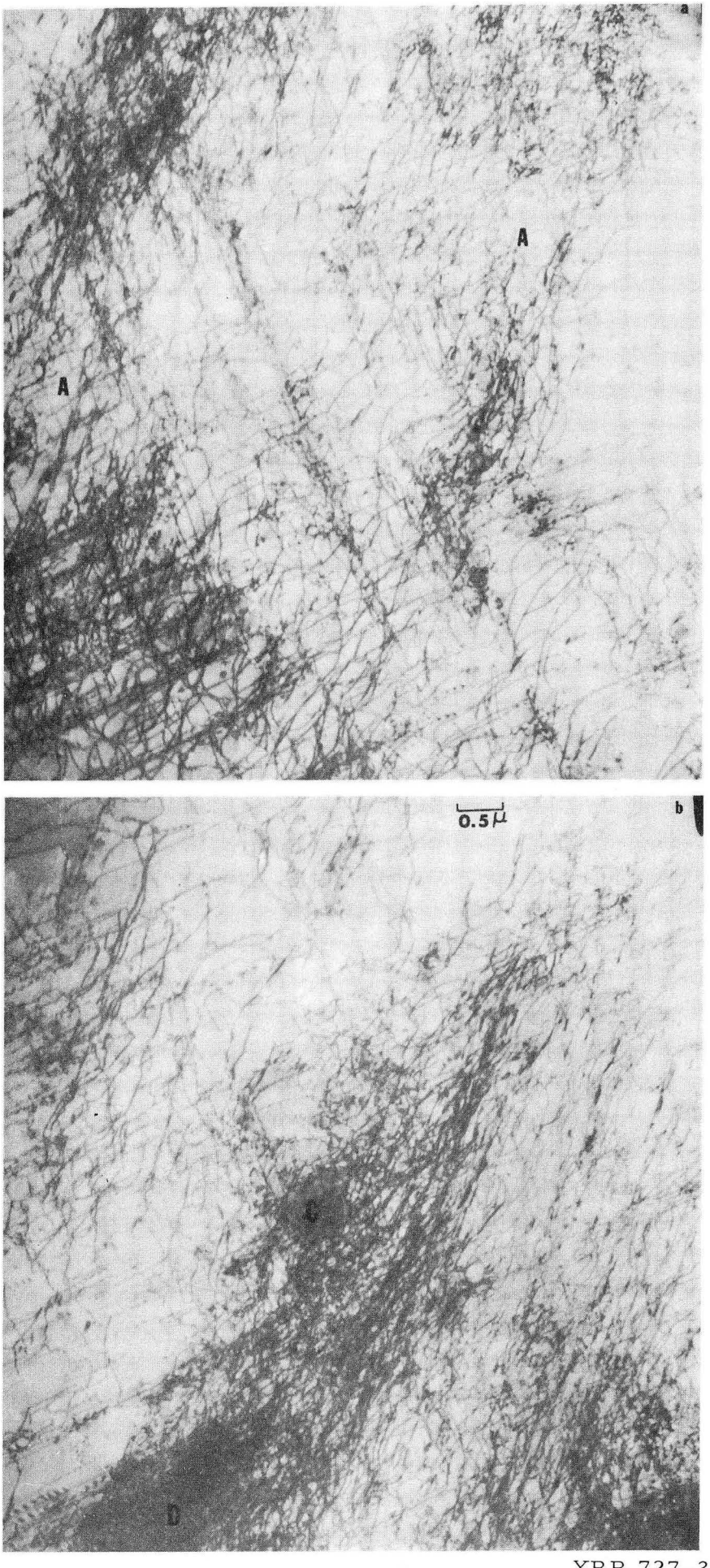

XBB 727-3651

Fig. 6.

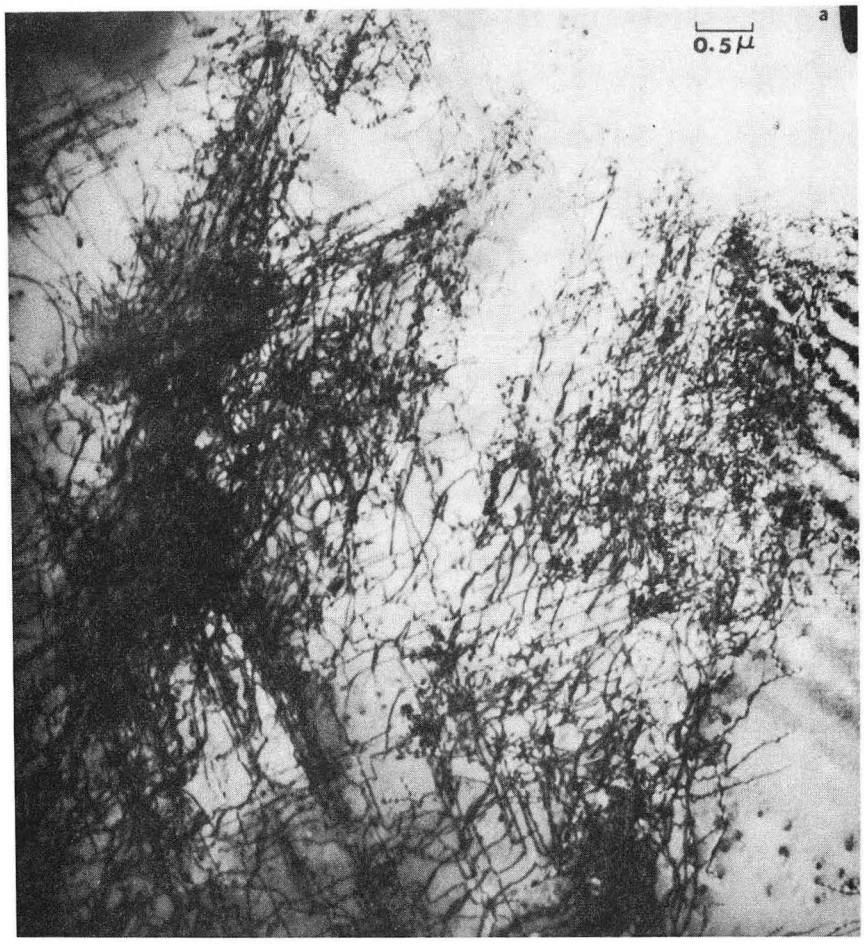

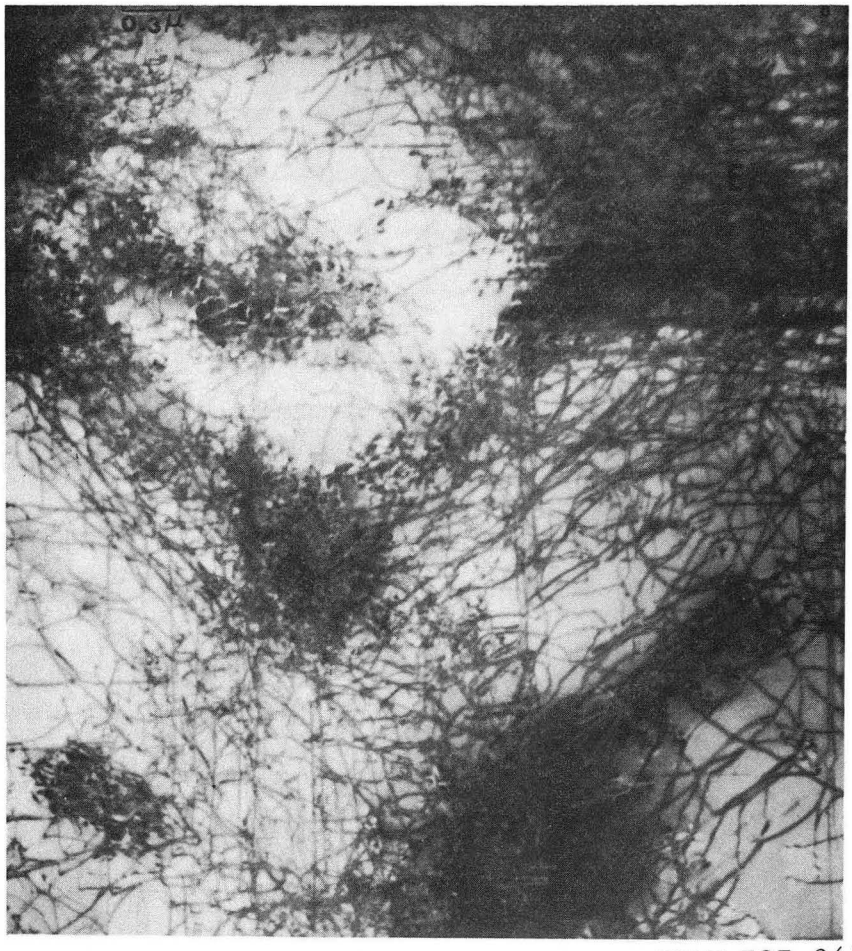

XBB 727-3650

Fig. 7.

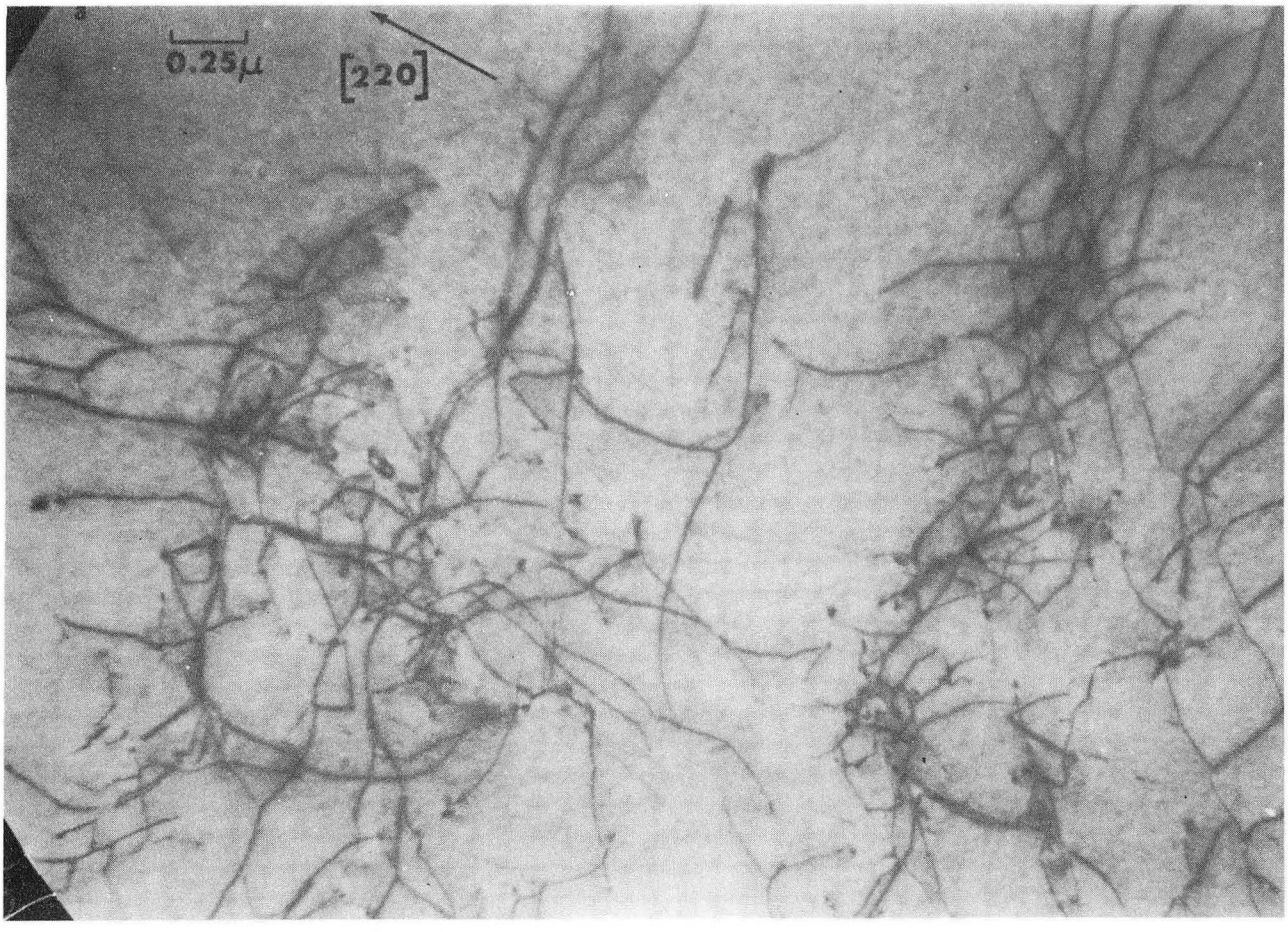

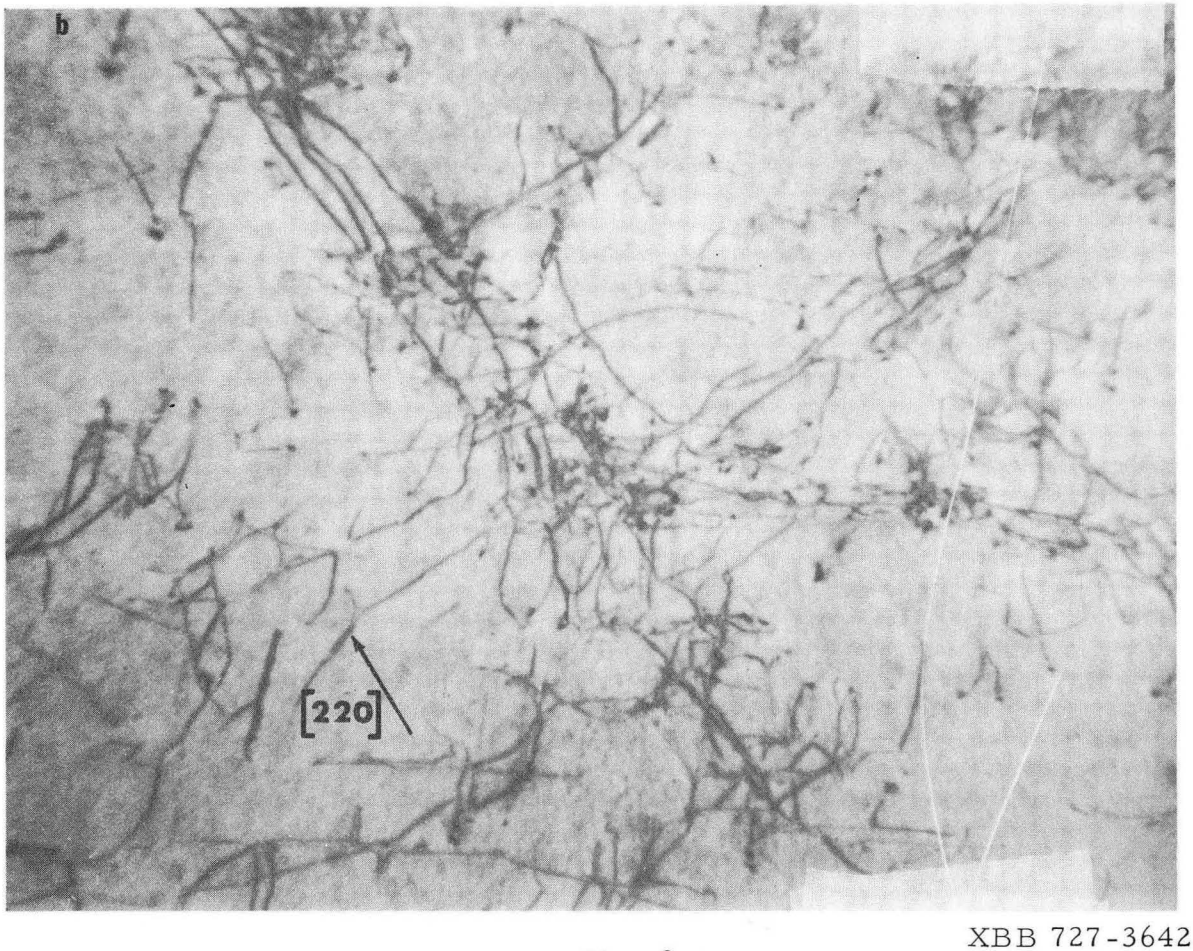

XBB 727-3642

Fig. 8.

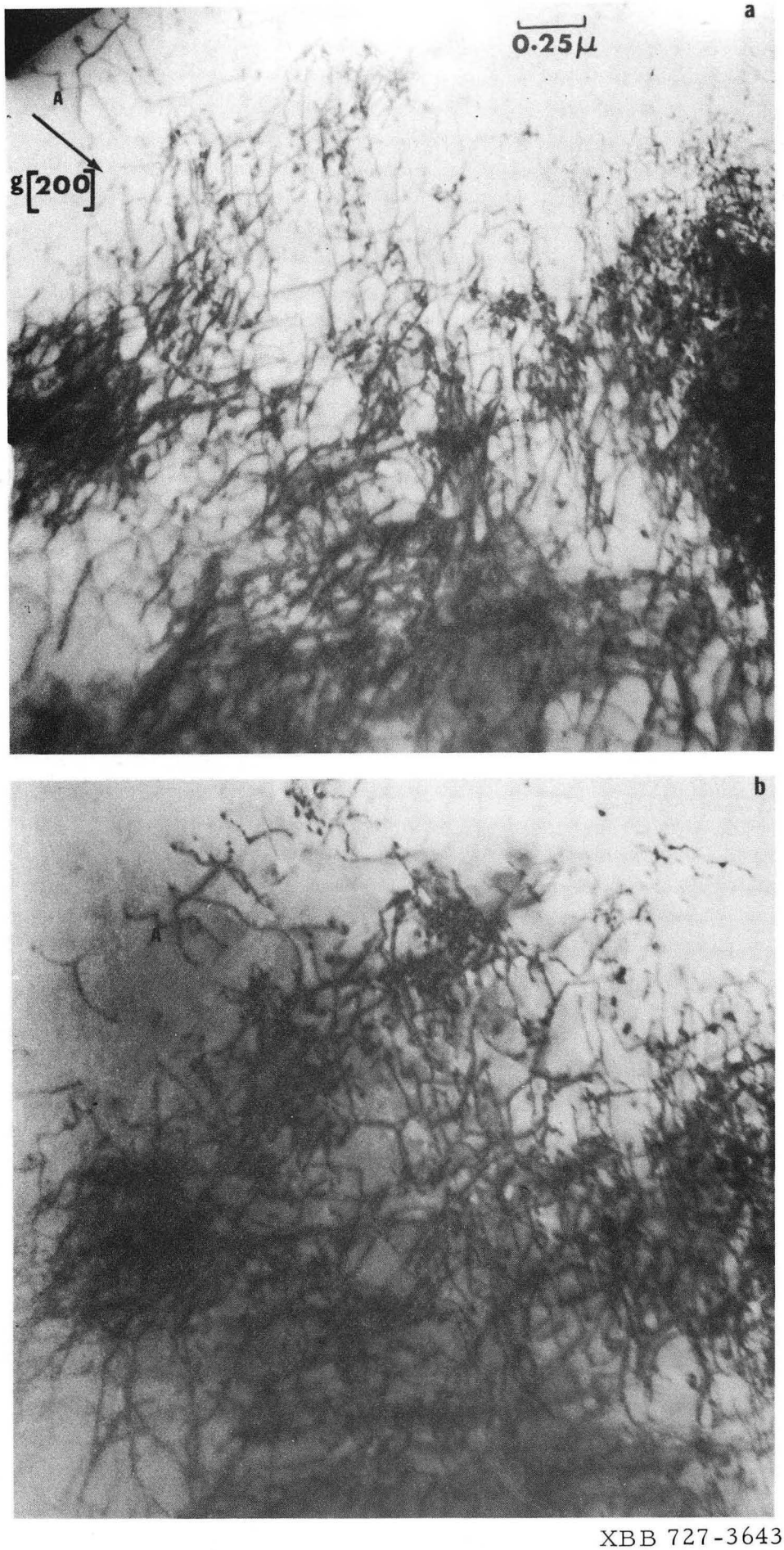

XBB 727-3643

Fig. 9.

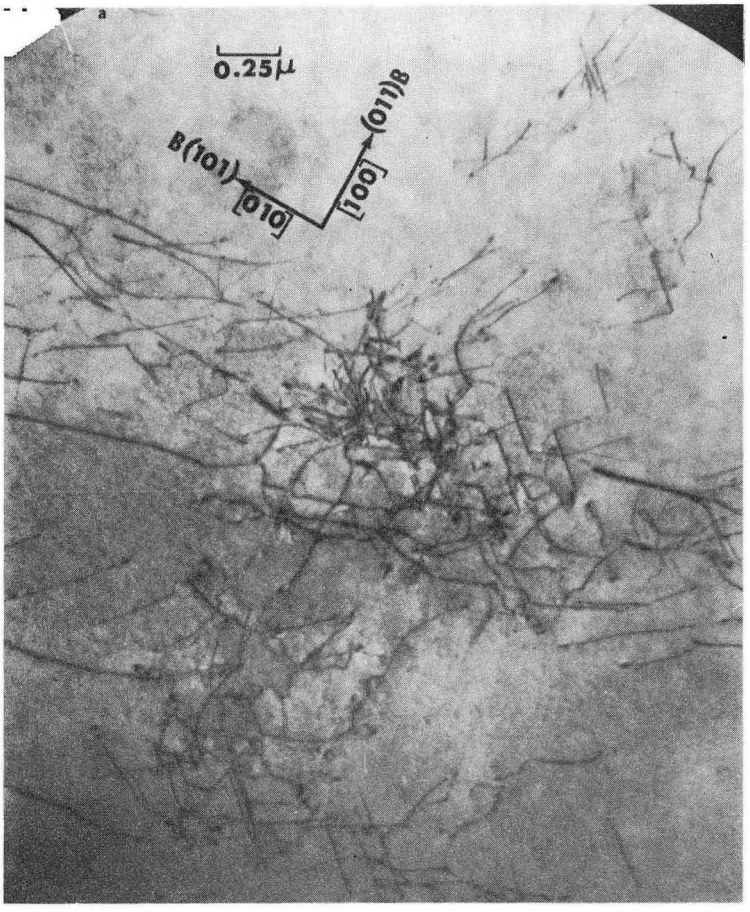

XBB 727-3647

Fig. 10.

XBB 727-3649

Fig. 11.

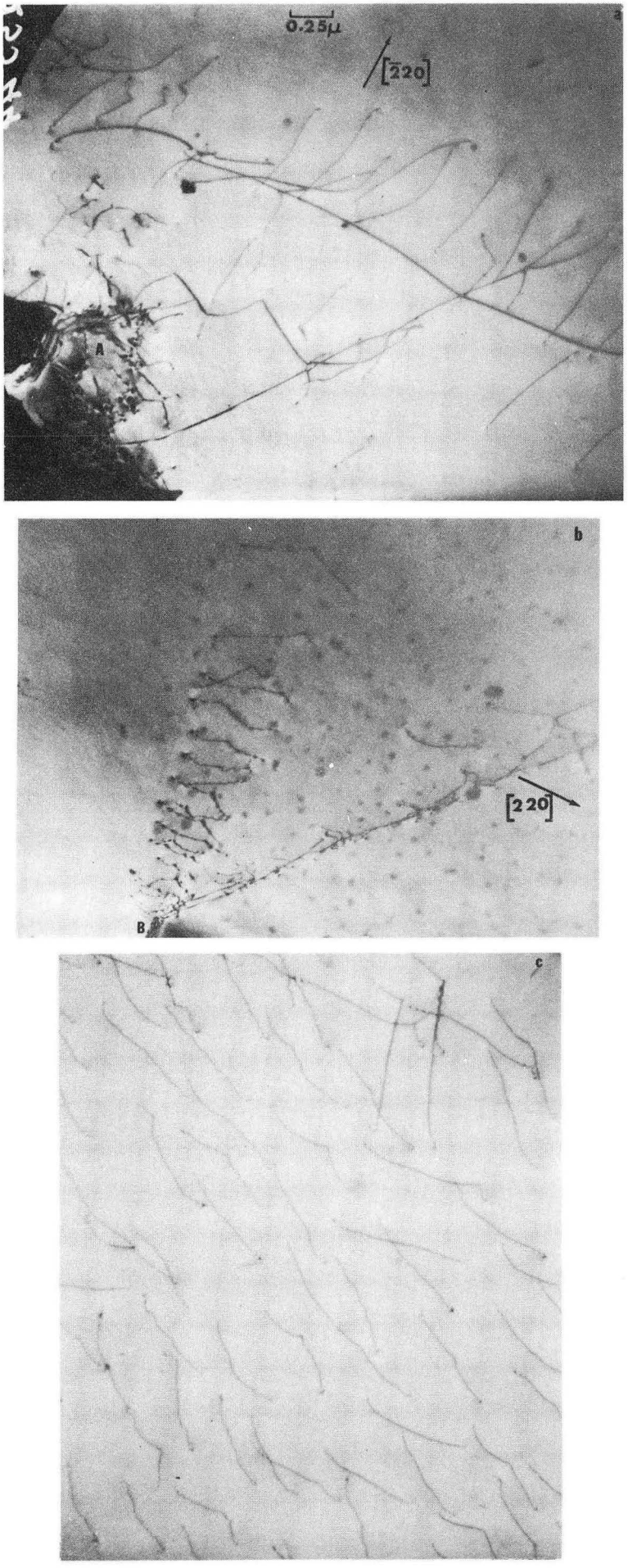

XBB 727-3648

Fig. 12.

TECHNICAL INFORMATION DIVISION
LAWRENCE BERKELEY LABORATORY
UNIVERSITY OF CALIFORNIA
BERKELEY, CALIFORNIA 94720